Journal of Alloys and Compounds 509 (2011) 7493–7497

Contents lists available at ScienceDirect

Journal of Alloys and Compounds

journal homepage: www.elsevier.com/locate/jallcom

Spectroscopic and magnetic investigation of NiCo nanoferrites

Asghari Maqsood [a,*], Kishwar Khan [a], M. Anis-ur-Rehman [b], M.A. Malik [b]

[a] Thermal Transport Laboratory, School of Chemical and Materials Engineering (SCME), National University of Sciences and Technology (NUST), H-12, Islamabad, Pakistan
[b] Applied Thermal Physics Laboratory, COMSATS Institute of Information Technology, Islamabad, Pakistan

ARTICLE INFO

Article history:
Received 15 February 2011
Received in revised form 15 April 2011
Accepted 16 April 2011
Available online 23 April 2011

Keywords:
Nanoparticles
Spectroscopic properties
Absorption bands
Magnetic measurements

ABSTRACT

Spectroscopic and magnetic characterization of $Ni_{1-x}Co_xFe_2O_4$ ($0.0 \le x \le 0.5$) nanoparticles is presented. The infrared spectra are measured in the frequency range 700–350 cm^{-1}. Two prominent bands are observed, low frequency band at about 400 cm^{-1} and high frequency band at about 600 cm^{-1} assigned to octahedral and tetrahedral sites, respectively. The force constants K_o and K_t corresponding to octahedral and tetrahedral sites, respectively are also calculated from FTIR spectra. The effect of co-concentration on the magnetic properties has been investigated using a vibrating sample magnetometer (VSM). After appropriate treatments, it is found that both magnetic saturation (M_s) and coercivities (H_c) increase with co-concentration.

1. Introduction

Mixed metallic oxides especially spinels having the general formula AB_2O_4 are very important materials for their technological applications. Spinel type nanoferrites have become more useful because of their chemical properties, optical and dielectric application such as in advanced microelectronics and dynamic random access memories (DRAMs) compared with their bulk counterparts [1,2]. $NiFe_2O_4$ is one of the most important spinel ferrite. It has cubic inverse spinel structure showing ferrimagnetism that originates from magnetic moment of anti-parallel spins between Fe^{3+} ions at tetrahedral sites and Ni^{2+} ions at octahedral sites. Many efforts have been done to increase the basic properties of ferrites by adding various ions of different valence states depending on the applications of interest [1]. The spectroscopic properties of ferrites are dependent on several factors such as preparation method, sintering process, etc. From application point of view, ferrite nanoparticles have unique properties and have promising technological applications in high-density magnetic recording, color imaging, ferrofluids, microwave devices, refrigerators, etc. Nanoparticles of spinel ferrites are also widely used as contrasting agents in magnetic resonance imaging (MRI), replacement of radioactive materials used as tracers and delivery of drugs to specific areas of the body [2]. Nowadays, the development of nano sized materials, in multilayer for spintronics or in aqueous suspensions for imaging or hyperthermia treatment of cancer cells has opened new fields of applications. This applied field requires great effort in chemical synthesis to control the composition, the morphology of nanostructures, and to investigate and develop new materials [3]. Further Ni–Co ferrites show a good magnetostrictive material into highly resistive Ni ferrite is one of the important phases for studying of this challenging material. Therefore by keeping this idea in our mind, we decided to study on the spectroscopic and magnetic analysis of Ni–Co ferrite with the above mentioned composition prepared by co-precipitation method. Many researchers studied the spinel ferrites MFe_2O_4 ferrites (where M is a divalent atom like Zn, Mg, Mn, Co, Ni, etc.) [4–6]. Cations distribution in spinel ferrites depends on many factors, such as ionic radii and electronic configuration. This distribution affects the microstructure and the magnetic properties of these ferrites. The effect of the cations distribution on spinel ferrites is studied widely and their structural and magnetic properties are also reported [7–9]. In the present work, we report the effect of Co substitution on the structural and magnetic properties of nickel spinel ferrite.

2. Experimental methods

The polycrystalline powders of series $Ni_{(1-x)}Co_{(x)}Fe_2O_4$ ($0.0 \le x \le 0.5$) were prepared by the chemical co-precipitation route and sintered for 8 h at 800 °C. The detail study about synthesis is already published by the same authors [10]. The chemical structure of the samples was determined from the X-ray diffraction (XRD) technique. The XRD patterns were recorded using CuKα radiation at room temperature, the X-ray powder diffraction patterns were taken in the range of 20–70°, 0.25/min in steps of 0.02 shown in Fig. 1. The FTIR spectra were recorded using Perkin Elmer Spectrum 100 FTIR Spectrometer, UK. The samples were prepared using KBr: ferrites with 100:1 ratio. The spectra were recorded in the range of 350–700 cm^{-1} at room temperature.

* Corresponding author. Tel.: +92 51 90855203, fax: +92 51 90855002.
E-mail addresses: tpl.qau@usa.net (A. Maqsood), kishwar.nust@gmail.com (K. Khan).

0925-8388/$ – see front matter © 2011 Elsevier B.V. All rights reserved.
doi:10.1016/j.jallcom.2011.04.092

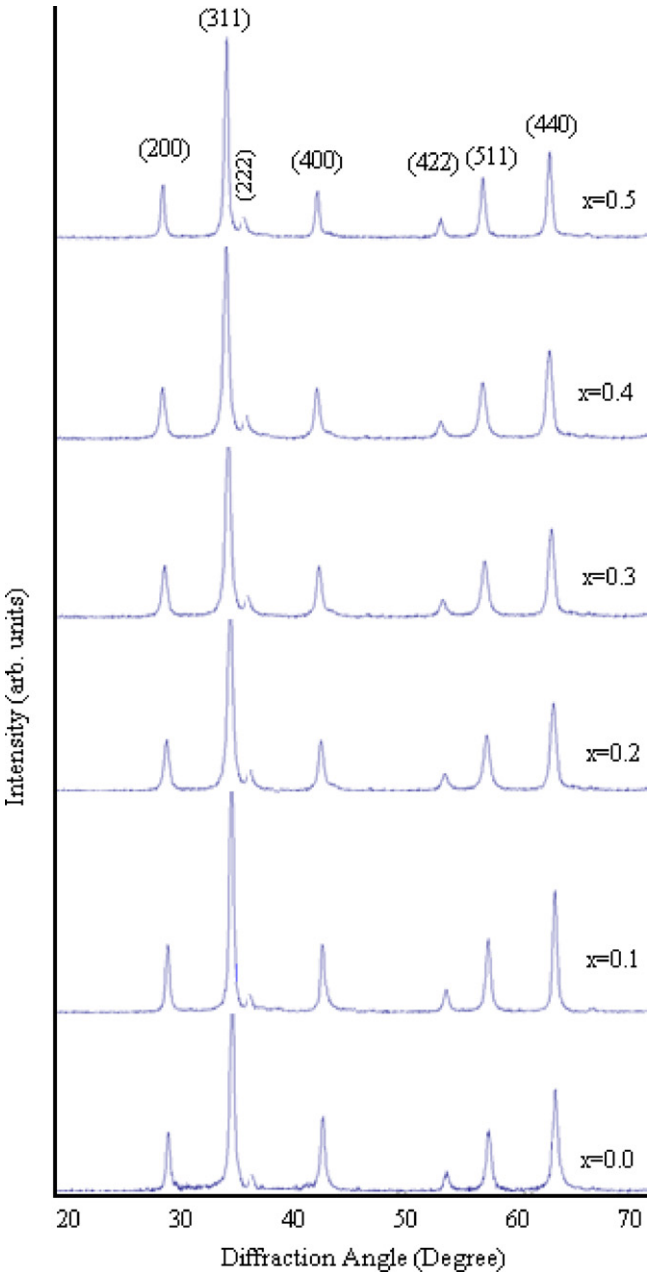

Fig. 1. X-ray diffraction pattern of $Ni_{(1-x)}Co_{(x)}Fe_2O_4$.

We measured the room temperature magnetic hysteresis for Ni–Co ferrite, similar work has also been reported for different spinel ferrites [11–17]. The hysteresis loops for the samples ($x = 0.1, 0.3, 0.5$) are shown in Fig. 3. The maximum applied magnetic field used in our study was (20 kOe). From the measured loops [18,19] we obtained the magnetic parameters M_s and H_c.

3. Results and discussions

3.1. X-ray diffractionation

Fig. 1 shows X-ray diffraction patterns for nanoferrites with $Ni_{1-x}Co_xFe_2O_4$ ($0.0 \le x \le 0.5$). The observed peaks for the plans 220, 311, 222, 400, 422, 511 and 440 confirmed the phase formation of $NiFe_2O_4$ with cubic spinel structure. The lattice parameter 'a' was calculated using the well known relation ($a = d(h^2 + k^2 + l^2)^{1/2}$). The results show that the lattice parameters slightly increase with the co-concentration in the lattice as shown in Table 1. The increase in 'a' with 'x' can be explained on the basis of difference in ionic radii of Ni and Co. The larger ionic radii of Co (0.72 Å) replaced the smaller ionic radii of Ni (0.69 Å), consequently the lattice parameter increased due to an expansion in the unit cell. Since each unit cell of the spinel ferrites contains 8 molecules, the value of X-ray density was determined according to the relation ($D_x = 8M/Na^3$) [10], where N is the Avogadro's number and M is the molecular weight of the sample. The mass density (D_m) was determined from mass and the bulk volume of the sample. The porosity (P) of the samples was calculated from D_x and D_m values using the expression ($P = (1 - D_m)/D_x$). Table 1 shows the values of D_m, D_x and P as a function of Co ion contents. The increase in both D_m and D_x can be attributed to the ionic radii mainly, since the atomic weights of Ni and Co are almost comparable. The porosity decreased with the Co-concentration. The approximate crystallite size (t) of the particle was determined from XRD broadening of the (3 1 1) peak using Scherrer formula ($t_{hkl} = 0.9\lambda/\beta\cos\theta$) [15], where, t_{hkl} is the mean dimension of the crystal perpendicular to the plane (hkl), β is the full width at half maximum in radians, θ is the Bragg's angle for the actual peak. Again the crystallite size obtained from Scherrer formula is tabulated in Table 1. It is noted that the crystallite size increased with the Co-concentration in the lattice.

Both $NiFe_2O_4$ and $CoFe_2O_4$ ferrites are inverse spinel [15], so the cation distribution in nickel cobalt ferrite can be expressed as:

$$[Co_t^{2+}(Fe_{1-t})]_A^{3+}[(Ni_{1-x})^{2+}(Co_{x-t})(Fe_{1+t})^{3+}]_B\,(O)^{2-}$$
$$\{0 \le x \le 0.5,\ 0 \le t \le 0.05\} \quad (1)$$

As Co^{2+} ions inserted in nickel ferrite, some of Co^{2+} cations can be migrated from (octahedral) to A-site (tetrahedral) [15].

Both the ionic radius of A-site (r_A) and B-site (r_B) can be determined using the cation distributions formulae.

$$r_A = tr_{Co} + (1 - t)\, r_{Fe} \quad (2)$$

$$r_B = \frac{1}{2}[(1 - x)r_{Ni} + (x - t)r_{Co} + (1 + t)\, r_{Fe}] \quad (3)$$

where 'x' is the concentration of Co^{2+} ions in the octahedral site and 't' takes the values from 0 to 0.05 [20].

3.2. FTIR studies

The infrared/IR spectra can provide information about the absorption bands arising from inter atomic vibrations. From these data, it is possible in principle to calculate force constants for the structure of bonds between octahedral or tetrahedral metal ions and oxide ions [21], the structural changes brought by the metal ions that are either lighter or heavier than divalent ions in the ferrites strongly influence the lattice vibration. Also the lattice vibration depends upon the cations mass, the cation oxygen and the bonding force. Spectra of $Ni_{1-x}Co_xFe_2O_4$ ($0.0 \le x \le 0.5$) in the range 350–700 cm^{-1} at room temperature are shown in Fig. 2. An inspection of the spectra shows two absorption bands, a common feature of all the ferrites [22]. The bands arise from lattice vibration of the oxide ions against the cations. The two main absorption bands υ_1 and υ_2 corresponding to the stretching vibration of the tetrahedral and octahedral sites [23,24] are around 600 and 400 cm^{-1}, respectively. The spectra show a shift due to the introduction of Co^{2+} ions in place of Ni^{2+}. The tetrahedral site bands are shifted from lower band value to higher band value i.e., 589–603 cm^{-1}, that can be attributed to the shifting of Fe^{3+} ions towards oxygen ion on occupation of tetrahedral site by Co^{2+} ions with larger ionic radii, which decrease the Fe^{3+}–O^{2-} distances. The octahedral site band varies between 387 cm^{-1} and 409 cm^{-1}. The values of

Table 1
The crystallite size t_{hkl} for (3 1 1) peak, XRD lattice parameters (a_{exp}), lattice volume (V), mass density (D_m), X-ray density (D_x), porosity (P), ionic radii of A (r_A) and B (r_B) sites for $Ni_{(1-x)}Co_{(x)}Fe_2O_4$ nanoferrites.

Parameters	Cobalt concentration (x)					
	$x=0.0$	$x=0.1$	$x=0.2$	$x=0.3$	$x=0.4$	$x=0.5$
t (3 1 1) (nm)	17	21	15	25	23	33
a_{exp} (Å)	8.335	8.341	8.342	8.344	8.345	8.346
V (Å^3)	579	580	580	581	581	581
D_m (g/cm^3)	2.79	2.88	2.98	3.2	3.47	3.52
D_x (g/cm^3)	5.37	5.36	5.36	5.36	5.36	5.35
P (fraction)	0.48	0.46	0.44	0.4	0.35	0.34
r_A (Å)	0.6400	0.6408	0.6416	0.6424	0.6440	0.6432
r_B (Å)	0.665	0.6662	0.6672	0.6705	0.6694	0.6683

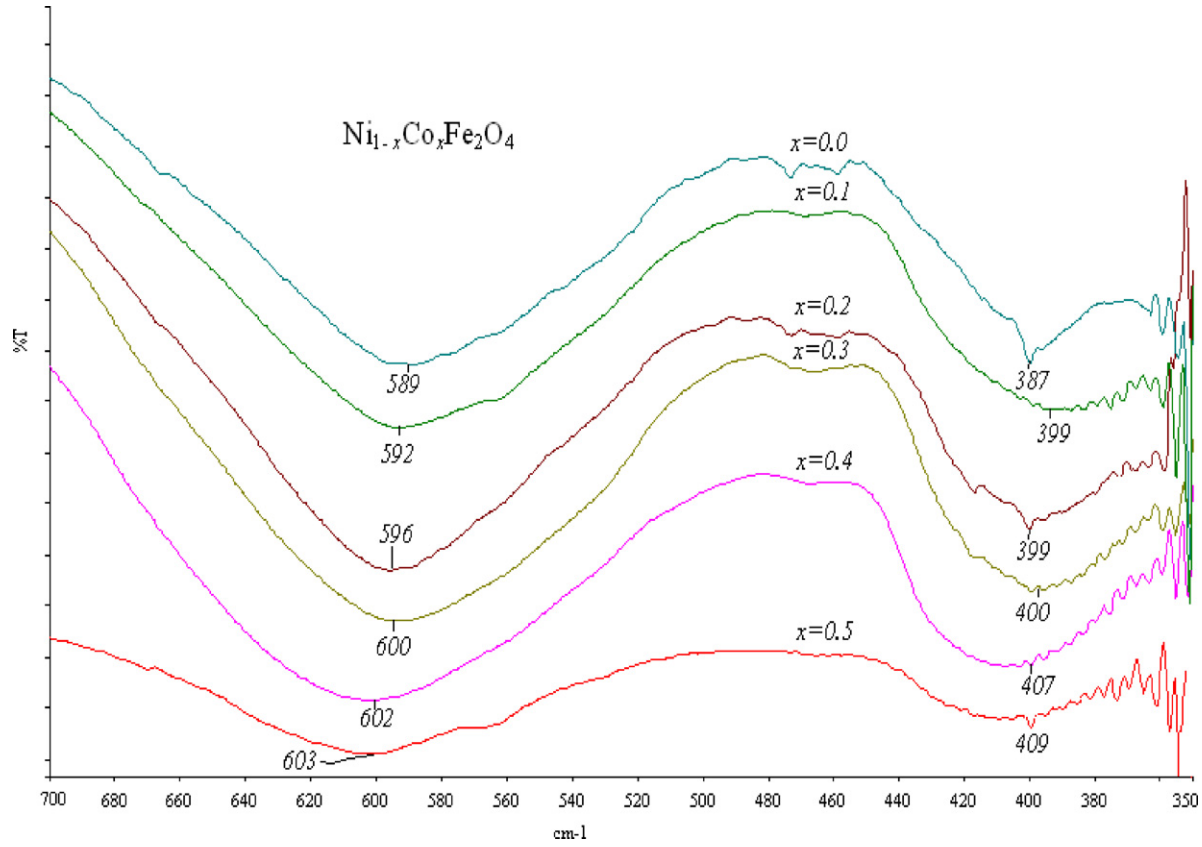

Fig. 2. FTIR spectra for $Ni_{(1-x)}Co_{(x)}Fe_2O_4$.

bond length for each composition are calculated according to the following relations [24] and are tabulated in Table 2.

$$R_A = a\sqrt{3}\left(\delta + \frac{1}{8}\right) \quad (4)$$

$$R_B = a\left(\frac{1}{16} - \frac{\delta}{2} + 3\delta^2\right)^{1/2} \quad (5)$$

From Table 2, it is evident that bond length of A-site is less than that of B-site. The force constants K_o and K_t corresponding to octahedral and tetrahedral vibrations, respectively have been obtained from the IR absorption data using the standard formula [21] as follows.

$$K_o(\text{dynes cm}^{-1}) = \frac{0.942128(M_1 \upsilon_2{}^2)}{M_1 + 32} \quad (6)$$

Table 2
FTIR related data and calculated parameters.

Parameters	Cobalt concentration (x)					
	$x=0.0$	$x=0.1$	$x=0.2$	$x=0.3$	$x=0.4$	$x=0.5$
υ_1 (cm^{-1})	589	592	596	600	602	603
υ_2 (cm^{-1})	387	399	399	400	407	409
R_A (Å)	1.9591	1.9631	1.9645	1.9650	1.9652	1.9655
R_B (Å)	1.9963	1.9977	1.9979	1.9983	1.9784	1.9988
$K_t \times 10^5$ dynes cm^{-1}	1.93074	2.00508	2.0223	2.0450	2.0918	2.10966
$K_o \times 10^5$ dynes cm^{-1}	0.897025	0.95558	0.95732	0.96403	1.00000	1.01182

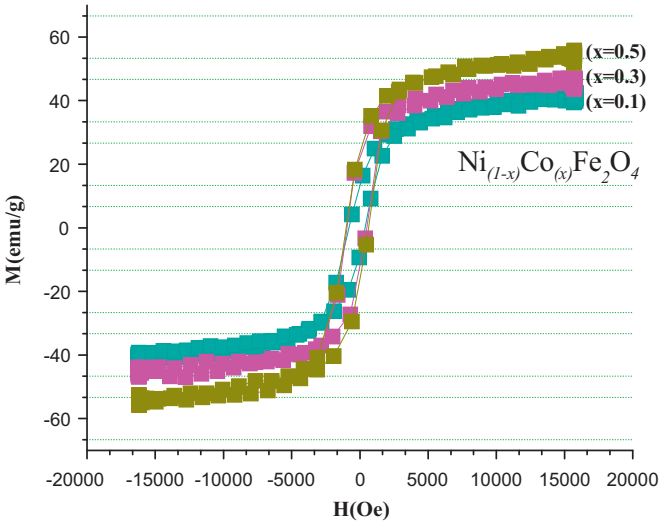

Fig. 3. M–H loops of $Ni_{(1-x)}Co_{(x)}Fe_2O_4$.

$$K_t(\text{dynes cm}^{-1}) = K_o \frac{\upsilon_1\sqrt{2}}{\upsilon_2} \quad (7)$$

where K_o is the force constant on octahedral site, K_t is the force constant on tetrahedral site, M_1 is the molecular weight of tetrahedral site, υ_1 is the corresponding center frequency on tetrahedral site, υ_2 is the corresponding center frequency on octahedral site. The molecular weight M_1 is calculated from the cation distribution. It is noted that the force constants increased with increase in bond lengths.

3.3. Magnetic characterization

The hysteresis loops obtained are shown in Fig. 3. The narrow loops for $Ni_{1-x}Co_xFe_2O_4$ ($x = 0.1, 0.3, 0.5$) samples indicate the soft nature of the ferrite nano materials. All the curves behave normally, the magnetization increased with increasing the applied magnetic field. Various magnetic properties such as saturation magnetization (M_s) and coercivity (H_c) are obtained from the hysteresis loops. The saturation magnetization (M_s) for each sample was determined by the magnetization curve at H_{max}. The values of saturation magnetization (M_s), magnetic moments (n_B) and coercivities (H_c) for various Co concentrations of Ni–Co nanoferrites are tabulated in Table 3 which is comparable with [18,19,25]. It is noticed that saturation magnetization (M_s) and coercivities (H_c) increased with $Co_{(x)}$. Similar results are reported by Skomski and Sellmyer [26]. The M–H curves show that magnetization is completely saturated around 15 kOe, this is due to the small size of the particles. The average particle size varies from 16 to 45 nm in our case [27]. There will be a size distribution allowing smaller particles to exist even when the average size is large. For such particles, the magnetic moments will fluctuate due to thermal energy reducing the overall magnetization. As the applied field increases, the fluctuations gradually decrease showing slight increase even at high fields. A similar observation is reported by Singh et al. [28]. The variation of saturation magnetization with $Co_{(x)}$ has an increasing trend [25]. From Table 3 it is seen that n_B increased with Co concentration in the lattice. The experimental values of the magnetic moment were calculated from the relation [15].

Table 3
Magnetic parameters of $Ni_{(1-x)}Co_{(x)}Fe_2O_4$.

Parameters	Cobalt concentration (x)		
	$x = 0.1$	$x = 0.3$	$x = 0.5$
M_s (emu g^{-1})	40	47	54
H_c (Oe)	596	712	851
n_B (μ_B)	0.907	1.183	1.497
α_{Y-K} (°)	27.58	42.58	52.05

$$n_B = M_{wt} \times \frac{\sigma_S}{5585} \times D_m \quad (8)$$

where M_{wt} the molecular weight of the sample and 'D_m' is the density of the sample, σ_S was calculated using the formula [29,30].

$$\sigma_S = (1 - P)M_s \times D_m \quad (9)$$

where P is the porosity and M_s is the saturation magnetization in emu g^{-1} taken from M–H loops as shown in Fig. 3.

The Yafet–Kittel (Y–K) angles have been calculated using the formula [30]

$$n_B = (6 + x)\cos\ \alpha_{(Y-K)} - 5(1 - x) \quad (10)$$

where x represents the substituting element. In case of Ni–Co ferrites, Y–K angles are due to the canted behavior of ions on the octahedral lattice site [31]. Again $\alpha_{(Y-K)}$ are shown in Table 3.

4. Conclusions

$Ni_{1-x}Co_xFe_2O_4$ ($0 \le x \le 0.5$) nano particles were successfully synthesized with various crystallite sizes depending on the thermal treatment and composition using the co-precipitation method. The cation distribution has been estimated by X-ray diffraction. The process of functional group has been identified by Fourier transform infrared (FTIR) spectra and the force constants are calculated from these spectra. All the samples in question presented very narrow (M_s) as a function of (H_c) loops, which is the characteristic of soft magnetic materials. In addition, increasing the $Co_{(x)}$ concentration in the system was found to increase the saturation magnetization and the coercivity.

Acknowledgements

The authors specially acknowledge Ms. Ghazala for her moral support. The financial support of Pakistan Science Foundation (PSF) through project no. Res/c-NUST. 147 is also acknowledged.

References

[1] Y.M. Al Anagri, J. Magn. Magn. Mater. 323 (2011) 1835–1839.
[2] K. Maaz, A. Mumtaz, S.K. Hasanain, A. Ceylan, J. Magn. Magn. Mater. 308 (2007) 289–295.
[3] C. Lefever, F. Roulland, N. Virat, J.M. Grenecence, G. Pourry, J. Solid State Chem. 183 (2010) 2623–2630.
[4] A. Ceylan, S. Ozcan, C. Ni, S.I. Shah, J. Magn. Magn. Mater. 320 (2008) 857.
[5] M.A. Elkestawy, J. Alloys Compd. 492 (2010) 616–620.
[6] M.G. Naseri, E.B. Saion, H.A. Ahangar, M. Hashim, A.H. Shaari, J. Magn. Magn. Mater. 323 (2011) 1745–1749.
[7] M. Al-Haj, J. Magn. Magn. Mater. 299 (2006) 435.
[8] M. Al-Haj, Turk. J. Phys. 29 (2005) 85.
[9] A.A. Sattar, H.M. El-Sayed, K.M. El- Shokrofty, M.M. El-Tabey, J. Appl. Sci. 5 (2005) 162.
[10] A. Maqsood, K. Khan, M.A. Rehman, M.A. Malik, J. Supercond. Nov. Magn. (2010), doi:10.1007/s10948-010-0956-9.
[11] A. Al-Sharif, M. Abo-AlSondos, Jordan J. Phys. 1 (2008) 61–72.
[12] M. Naeem, N.A. Shah, I.H. Gul, A. Maqsood, J. Alloys Compd. (2009) 487–739.
[13] R.S. Devan, Y.R. Ma, B.K. Chougule, Mater. Chem. Phys. 115 (2009) 263–268.
[14] C. Caizer, M. Stefanescua, C. Munteana, I. Hrianca, J. Electr. Adv. Mater. 3 (2001) 919–924.
[15] J. Smit, H.P.J. Wijin, Ferrites, Wiley, New York, 1959.
[16] Y. Köseoğlu, A. Baykal, F. Gözüak, H. Kavas, Polyhedron 28 (2009) 2887–2892.
[17] M.M. Eltabey, J. Mater. Sci.: Mater. Electron. (2010) 221–229.
[18] S. Singhal, J. Singhal, S.K. Barthwal, K. Chandra, J. Solid State Chem. 178 (2005) 3183–3189.
[19] K. Maaz, W. Khalid, A. Mumtaz, S.K. Hasanain, J. Liu, J.L. Duan, Physica E 41 (2009) 593–599.
[20] H.M. Zaki, S.F. Mansour, J. Phys. Chem. Solids 67 (2006) 1643.
[21] R.D. Waldran, Phys. Rev. 99 (1955) 1727.

[22] C.G. Ramankutty, S. Sugunan, Appl. Catal. A: Gen. 218 (2001) 39–51.
[23] A. Adam, Z. Ali, E. Abdeltwab, Y. Abbas, J. Ovonic Res. 5 (2009) 157–165.
[24] K.J. Standley, Oxide Magnetic Materials, Oxford University Press, London, 1962, p. 962.
[25] J. Azadmanjiri, Mater. Chem. Phys. 109 (2008) 109–112.
[26] R. Skomski, D.J. Sellmyer, Handbook of Advanced Magnetic Materials, Advanced Magnetic Materials, vol. 1, Tsinghua University Press, Beijing, 2005, p. 30.
[27] A. Maqsood, K. Khan, J. Alloys Compd. 509 (2011) 3393–3397.
[28] R.K. Singh, A. Yadav, K. Prasad, A. Narayan, Int. J. Eng. Sci. Technol. 2 (2010) 73–79.
[29] G.K. Joshi, A.Y. Khot, S.R. Swant, Solid State Commun. 65 (1988) 1593.
[30] S.S. Bellad, R.B. Pujar, B.K. Chougule, Mater. Chem. Phys. 52 (1998) 166.
[31] Y. Yafet, C. Kittel, Phys. Rev. 90 (1952) 295.